PHYSICAL REVIEW C VOLUME 35, NUMBER 3 MARCH 1987

Test of the triaxial rotor model and the interacting boson-fermion approximation model description of collective states in ^{193}Ir

F. K. McGowan, N. R. Johnson, I. Y. Lee, W. T. Milner, and C. Roulet*
Oak Ridge National Laboratory, Oak Ridge, Tennessee 37831

R. M. Diamond and F. S. Stephens
Lawrence Berkeley Laboratory, Berkeley, California 94720

M. W. Guidry
University of Tennessee, Knoxville, Tennessee 37916
and Oak Ridge National Laboratory, Oak Ridge, Tennessee 37831
(Received 20 June 1986)

Coulomb excitation of states in ^{193}Ir up to $J=\frac{21}{2}$ has been observed with 160-MeV ^{40}Ar and 617-MeV ^{136}Xe ions. Most of these states are grouped into three rotational-like bands based on the $\frac{3}{2}^+$ ground state, the $\frac{1}{2}^+$ first excited state, and the $\frac{7}{2}^+$ γ-vibrational-like state at 621 keV. The average deviation between experimental and theoretical energies for 18 states is 54 keV for the particle-asymmetric-rigid-rotor model and 66 keV for the interacting boson-fermion approximation model [limited to broken Spin(6) symmetry and only the $d_{3/2}$ orbital is considered]. The overall agreement of both model predictions with experimental γ-ray yields for the collective transitions within the $\frac{3}{2}^+$ band is quite good. For interband transitions originating in the $K=\frac{1}{2}^+$ and $\frac{7}{2}^+$ bands, the interacting boson-fermion approximation model tends to underestimate the γ-ray yields by one to two orders of magnitude. In ^{193}Ir there are eight $\Delta\tau_1 \geq 2$ and six $\Delta\sigma_1=1$ transitions which are forbidden in the U(6/4) and U(6/20) supersymmetry schemes. The interacting boson-fermion approximation model tends to underestimate the $B(E2)$ values of two of these transitions with moderate collectivity by at least one order of magnitude. The interband transition $\frac{3}{2}' \rightarrow \frac{3}{2}$ ($\Delta\tau_1=2$ transition) with moderate collectivity is not a special situation in ^{193}Ir but a general feature in ^{191}Ir and ^{197}Au. For the remainder of the forbidden transitions in the supersymmetry schemes, the experimental $B(E2)$ values are an order of magnitude smaller than the collective ones. Both supersymmetry schemes and the broken Spin(6) model reproduce the collective $E2$ transitions with $\Delta\tau_1=1$ reasonably well. The triaxial rotor model description of the experimental energies and the collective $E2$ transitions is the most successful approach. The $B(E3)$ for excitation of several negative-parity states in ^{193}Ir is $(3.3\pm2.0)B(E3)_{\rm sp}$.

I. INTRODUCTION

In a previous paper[1] we presented the results from Coulomb excitation of ^{191}Ir with 160-MeV ^{40}Ar and 617-MeV ^{136}Xe ions and compared these results with the predictions of two models, viz., the particle-asymmetric-rigid-rotor model[2] and the interacting boson-fermion approximation (IBFA) model.[3] The numerical calculations with the IBFA model included only the $d_{3/2}$ orbital but did allow for breaking of the Spin(6) symmetry. These results also tested the role of supersymmetry in this mass region.

Most of the states could be grouped into three rotational-like bands based on the $\frac{3}{2}^+$ ground state, the $\frac{1}{2}^+$ first excited state, and the $\frac{7}{2}^+$ γ-vibrational-like state at 686 keV in ^{191}Ir. Prior to this study, the experimental evidence presented in support of supersymmetry in the Os—Ir nuclei has been limited. The average deviation between experimental and theoretical energies for 20 states in ^{191}Ir is 45 keV for the particle-asymmetric-rigid-rotor model and 125 keV for the IBFA model. The overall agreement of both model predictions of the experimental γ-ray yields for the collective transitions within the $\frac{3}{2}^+$ band is quite good. For interband transitions originating in the $K=\frac{1}{2}^+$ and $\frac{7}{2}^+$ bands, the IBFA model tends to underestimate the γ-ray yields by one to two orders of magnitude. Six of these interband transitions correspond to $\Delta\tau_1=2$ transitions in the U(6/4) of U(6/20) supersymmetry schemes[4,5] and are forbidden in these schemes. Two of these transitions are moderately collective with $B(E2)$ values of 17 and 10 single particle units (s.p.u.). The broken Spin(6) calculations predict values of 2 and 1.2 s.p.u. For both supersymmetric schemes there is a lack of detailed agreement with the very collective $E2$ transitions which have $\Delta\tau_1=0,\pm1$. These features are, however, reproduced to a much better degree by the broken Spin(6) calculations. The most successful interpretation of the experimental energies of the states and the $B(E2)$ values in ^{191}Ir is the particle-asymmetric-rigid-rotor model.

In this paper we present a similar set of results from Coulomb excitation of ^{193}Ir and compare these results with the predictions of the two models mentioned above. These results also test the role of supersymmetry in describing the collective states in ^{193}Ir.

II. EXPERIMENTAL PROCEDURE AND RESULTS

Coulomb excitation of states in ^{193}Ir up to $J=\frac{21}{2}$ have been observed with 160-MeV ^{40}Ar ions from the Oak Ridge Isochronous Cyclotron (ORIC) and 617-MeV ^{136}Xe ions from the SuperHILAC. At ORIC the backscattered ^{40}Ar ions were detected in an annular solid-state surface-barrier detector in coincidence with γ rays detected in three Ge(Li) detectors. At the SuperHILAC the γ rays from Coulomb excitation were detected in two Ge(Li) detectors in coincidence with scattered projectiles and recoiling nuclei. These particles were detected in two parallel plate avalanche counters. Details related to target preparation (99.45% ^{193}Ir), detectors, calibrations, and experimental method may be found in Ref. 1.

The coincidence γ-ray spectra of ^{193}Ir are very similar to the spectra observed from Coulomb excitation of ^{191}Ir.[1] From our γ-ray spectra, the previously known decay scheme,[6] the (n,n'γ) reaction data,[7] and γ-ray decay systematics of ^{191}Ir, the transitions and γ-ray energies observed in the present experiments were placed in the level diagram shown in Fig. 1. Most of the states in ^{193}Ir are grouped into three rotational-like bands based on the $\frac{3}{2}^+$ ground state, the $\frac{1}{2}^+$ first excited state, and the $\frac{7}{2}^+$ γ-vibrational-like state at 621 keV. The new spin assignments, $J \geq \frac{7}{2}$, in these three bands come from the similarity of the γ-ray decay systematics of ^{191}Ir. The placement of the $\frac{9}{2}$ and $\frac{11}{2}$ states of the γ-vibrational-like band at 892 and 1169 keV is based primarily on γ-ray energy summation of several interband transitions. Although we observed states up to $J=\frac{13}{2}$ of the rotational-like band based on the $\frac{1}{2}^+$ first excited state in ^{191}Ir, we were unable to extend this band beyond $J=\frac{9}{2}$ in ^{193}Ir in spite of the doublet nature of the states J in the $\frac{3}{2}^+$ band and the states $J-1$ in the $\frac{1}{2}^+$ band. The state of 807 keV has only been seen before in the (n,n'γ) reaction.[7]

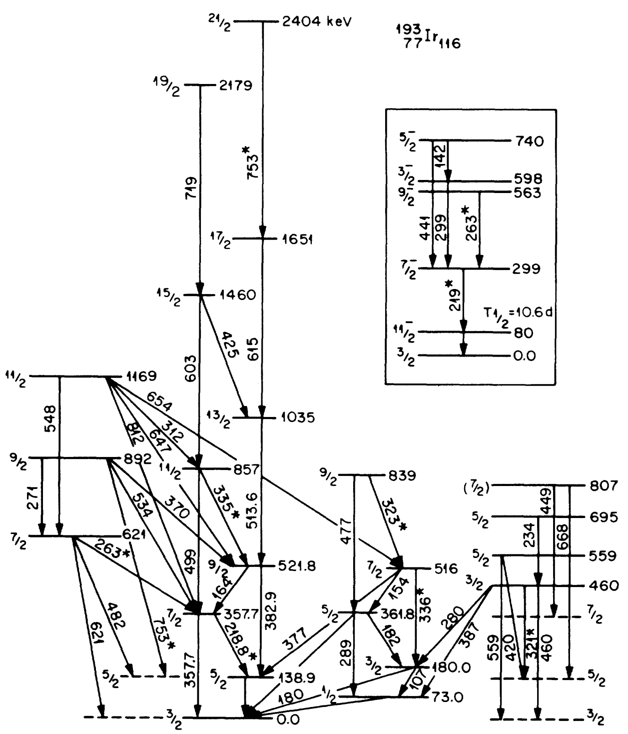

FIG. 1. Level diagram of positive parity states from Coulomb excitation and the γ-ray transitions from decay of these states. The transitions marked with an asterisk are placed more than once in the scheme. The inset contains the negative parity states which were populated. Only the transitions $\frac{1}{2}\rightarrow\frac{3}{2}$ of 73 keV and $\frac{5}{2}^-\rightarrow\frac{3}{2}^-$ of 142 keV were not observed in the present experiment.

The γ-ray yields from Coulomb excitation of ^{193}Ir are presented relative to the $\frac{7}{2}^+\rightarrow\frac{3}{2}^+$ transition of 357.7 keV in Table I. Yields of the corresponding transitions for ^{191}Ir are included to show the extreme similarity. This provided a basis for extending the rotational-like band built on the $\frac{3}{2}^+$ ground state to higher spins in ^{193}Ir. The correlation of the γ-ray yields in ^{191}Ir and ^{193}Ir also lends support for the placement of the levels in the other two rotational-like bands in ^{193}Ir. Entries marked with an asterisk are γ-ray transitions which are placed more than once in the level scheme of Fig. 1. The relative γ-ray yields from decay of the Coulomb excitation of states at 460, 559, 695, and 807 keV are tabulated in Table II. In addition to the positive parity states, several negative parity states appear to be Coulomb excited in ^{193}Ir with ^{136}Xe and ^{40}Ar ions (see inset of Fig. 1). These γ-ray yields are also given in Table I.

III. DISCUSSION

In the present experiment, the $E2$ matrix elements of higher spin states can be studied. However, because of the large number of bands and the number of paths by which a level can be excited, the number of matrix elements involved in the excitation is larger than the number of levels for which the yield is measured. Thus, a complete model independent analysis of the present data is not possible. But, by using the values of $E2$ matrix elements deduced from light-ion Coulomb excitation[6] and by using nuclear spectroscopic information for the decay modes of these states,[6] a model dependent analysis of the yields of the higher-lying states can be carried out.

We have compared the experimental results with the predictions of two models, viz., the particle-asymmetric-rigid-rotor model[2] and the IBFA model.[3] The Coulomb excitation yields were calculated with the Winther and deBoer[8] program. For the input of the program, we use the experimental level energies and a set of $E2$ matrix elements taken from calculations with the particle-triaxial-rigid-rotor model program.[9] Orbitals with sequence numbers[2] 19, 20, and 21, corresponding mainly to $\frac{5}{2}^+$[402], $\frac{1}{2}^+$[411], and $\frac{3}{2}^+$[402] Nilsson orbitals which arise from the $2d_{5/2}$ and $2d_{3/2}$ shell model orbitals, were included in

TABLE I. Relative γ-ray yields $\sum_{\theta_\gamma} I_\gamma(J_i \to J_f)/\sum_{\theta_\gamma} I_\gamma(\frac{7}{2} \to \frac{3}{2})$ for ^{191,193}Ir + 160-MeV ^{40}Ar and $I_\gamma(J_i \to J_f)/I_\gamma(\frac{7}{2} \to \frac{3}{2})$ for ^{191,193}Ir + 617-MeV ^{136}Xe. The unprimed, single-primed, and double-primed states refer to states in the $\frac{3}{2}^+$, $\frac{1}{2}^+$, and $\frac{7}{2}^+$ rotational-like bands, respectively. Gamma-ray transitions marked with an asterisk are placed more than once in the table.

		E_γ (keV)		$\sum_{\theta_\gamma} I_\gamma(J_i \to J_f)/\sum_{\theta_\gamma} I_\gamma(\frac{7}{2} \to \frac{3}{2})$		$I_\gamma(J_i \to J_f)/I_\gamma(\frac{7}{2} \to \frac{3}{2})$	
J_i	J_f	^{191}Ir	^{193}Ir	^{191}Ir	^{193}Ir	^{191}Ir	^{193}Ir
$\frac{21}{2}$	$\frac{17}{2}$	712	753*			0.132±0.024	(0.16±0.03)
$\frac{19}{2}$	$\frac{15}{2}$	694	719			0.164±0.027	0.084±0.019
$\frac{17}{2}$	$\frac{13}{2}$	595	615	0.017±0.003		0.63±0.09	0.69±0.06
$\frac{15}{2}$	$\frac{11}{2}$	586	603	0.055±0.006	0.033±0.004	0.74±0.06	0.47±0.04
$\frac{15}{2}$	$\frac{13}{2}$	414	425	0.017±0.003		0.095±0.019	0.050±0.017
$\frac{13}{2}$	$\frac{9}{2}$	501	514	0.20±0.01	0.153±0.008	1.58±0.11	1.5±0.11
$\frac{11}{2}$	$\frac{7}{2}$	489	499	0.393±0.012	0.335±0.013	1.20±0.09	1.08±0.08
$\frac{11}{2}$	$\frac{9}{2}$	330	335	0.139±0.007	0.086±0.018	0.155±0.022	0.20±0.05
$\frac{9}{2}$	$\frac{5}{2}$	373	383	1.16±0.03	0.89±0.03	2.49±0.16	2.17±0.15
$\frac{9}{2}$	$\frac{7}{2}$	159	164	0.103±0.006	0.100±0.007	0.16±0.02	0.16±0.02
$\frac{7}{2}$	$\frac{3}{2}$	343	358	1.00	1.00	1.00	1.00
$\frac{7}{2}$	$\frac{5}{2}$	214	219*	0.637±0.017	0.656±0.022	0.514±0.043	0.69±0.05
$\frac{5}{2}$	$\frac{3}{2}$	129	139	0.941±0.025	1.11±0.03	0.70±0.05	0.92±0.06
$\frac{13}{2}'$	$\frac{11}{2}'$	406				0.115±0.020	
$\frac{11}{2}'$	$\frac{7}{2}'$	487		0.037±0.007			
$\frac{9}{2}'$	$\frac{5}{2}'$	461	477	0.055±0.005	0.043±0.005	0.190±0.025	0.14±0.02
$\frac{9}{2}'$	$\frac{7}{2}'$	308	323	0.030±0.004	0.017±0.004	0.103±0.016	0.095±0.013
$\frac{9}{2}'$	$\frac{7}{2}$	469		0.022±0.004		0.116±0.021	
$\frac{7}{2}'$	$\frac{3}{2}'$	325	336	0.073±0.005	0.069±0.014	0.213±0.024	0.169±0.037
$\frac{7}{2}'$	$\frac{5}{2}'$	153	154	0.039±0.005	0.036±0.005	0.058±0.014	0.032±0.012
$\frac{7}{2}'$	$\frac{5}{2}$	375	377	0.038±0.008	0.121±0.008		0.29±0.03
$\frac{5}{2}'$	$\frac{1}{2}'$	268*	289	0.056±0.005	0.055±0.005	0.116±0.018	0.16±0.02
$\frac{5}{2}'$	$\frac{3}{2}'$	172	182	0.125±0.007	0.100±0.007	0.220±0.025	0.12±0.02
$\frac{5}{2}'$	$\frac{3}{2}$	351	362	0.105±0.006	0.120±0.008	0.196±0.024	0.25±0.03
$\frac{3}{2}'$	$\frac{1}{2}'$	97	107	0.065±0.013	0.065±0.009		
$\frac{3}{2}'$	$\frac{3}{2}$	179	180	0.044±0.004	0.046±0.005	0.098±0.020	0.086±0.017
$\frac{11}{2}''$	$\frac{7}{2}''$	521	548	0.021±0.003	0.021±0.004	0.127±0.021	0.179±0.036
$\frac{11}{2}''$	$\frac{7}{2}$		812				0.056±0.020
$\frac{11}{2}''$	$\frac{9}{2}$	704	647		0.030±0.005	0.080±0.021	0.107±0.022
$\frac{11}{2}''$	$\frac{11}{2}$		312				0.053±0.017
$\frac{11}{2}''$	$\frac{7}{2}'$		654				0.043±0.012
$\frac{9}{2}''$	$\frac{7}{2}''$		271		0.014±0.005		0.074±0.016
$\frac{9}{2}''$	$\frac{5}{2}$	817	753*	0.017±0.004	0.013±0.004	0.105±0.025	(0.16±0.03)
$\frac{9}{2}''$	$\frac{7}{2}$	603	534	0.024±0.004	0.023±0.04	0.221±0.032	0.12±0.02
$\frac{9}{2}''$	$\frac{9}{2}$	443	370	0.020±0.004	0.015±0.004	0.182±0.025	0.083±0.019

TABLE I. (*Continued.*)

J_i	J_f	E_γ (keV) ^{191}Ir	E_γ (keV) ^{193}Ir	$\sum_{\theta_\gamma} I_\gamma(J_i \to J_f) / \sum_{\theta_\gamma} I_\gamma(\frac{7}{2} \to \frac{3}{2})$ ^{191}Ir	$\sum_{\theta_\gamma} I_\gamma(J_i \to J_f) / \sum_{\theta_\gamma} I_\gamma(\frac{7}{2} \to \frac{3}{2})$ ^{193}Ir	$I_\gamma(J_i \to J_f)/I_\gamma(\frac{7}{2} \to \frac{3}{2})$ ^{191}Ir	$I_\gamma(J_i \to J_f)/I_\gamma(\frac{7}{2} \to \frac{3}{2})$ ^{193}Ir
$\frac{7}{2}''$	$\frac{3}{2}$	686	621	0.209±0.009	0.250±0.011	0.400±0.040	0.525±0.047
$\frac{7}{2}''$	$\frac{5}{2}$	557	482	0.276±0.008	0.335±0.013	0.209±0.025	0.352±0.033
$\frac{7}{2}''$	$\frac{7}{2}$		263*		0.039±0.005		0.135±0.018
$\frac{7}{2}^-$	$\frac{11}{2}^-$	220	219*	0.045±0.004		0.115±0.024	
$\frac{9}{2}^-$	$\frac{7}{2}^-$	263	263*	0.019±0.004		0.080±0.015	
$\frac{9}{2}^-$	$\frac{11}{2}^-$	483		0.024±0.003		0.150±0.024	
$\frac{3}{2}^-$	$\frac{7}{2}^-$	268*	299		0.020±0.004		
$\frac{5}{2}^-$	$\frac{7}{2}^-$	409	441				0.051±0.016

the calculations. The deformation parameters ϵ and γ were adjusted to give the best agreement between theoretical and experimental excitation energies. Figure 2 shows the theoretical levels for $\epsilon=0.15$, $\gamma=26°$, and $E(2^+)=210$ keV alongside the experimental levels for ^{193}Ir. The average absolute deviation between the experimental and theoretical energies is 54 keV for a fit to 18 states in ^{193}Ir. These parameters are similar to those for the $(A-1)$ core ^{192}Os, viz., $\epsilon=0.149$, $\gamma=25.1°$, and $E(2^+)=206$ keV. The other parameters in this model calculation are the strength parameters κ_p and μ_p of the $\mathbf{l}\cdot\mathbf{s}$ and $\mathbf{l}^2$ terms in the modified oscillator potential and the pairing strength parameters g_0 and g_1. The values of these parameters for the calculations are given in Ref. 1. A striking feature of the level schemes in Fig. 2 is the doublet nature of the states J in the $\frac{3}{2}^+$ band and the states $J-1$ in the $\frac{1}{2}^+$ band. This characteristic feature, approximate pseudospin symmetry, also occurs in ^{191}Ir.[1]

The $E2$ matrix elements from the IBFA model were obtained from a numerical calculation[10] which included only the $d_{3/2}$ orbital but did allow for breaking of the Spin(6) symmetry. This symmetry breaking was introduced in both the parameters of the boson core and the parameters of the boson-fermion interaction. The values of the parameters (ODDA code) used in the IBFA model calculations were

TABLE II. Relative γ-ray yields $\sum_{\theta_\gamma} I_\gamma(J_i \to J_f)/\sum_{\theta_\gamma} I_\gamma(\frac{7}{2} \to \frac{3}{2})$ for ^{193}Ir + 160-MeV ^{40}Ar and $I_\gamma(J_i \to J_f)/I_\gamma(\frac{7}{2} \to \frac{3}{2})$ for ^{193}Ir + 617-MeV ^{136}Xe.

J_i	J_f	E_γ (keV)	$\sum_{\theta_\gamma} I_\gamma(J_i \to J_f) / \sum_{\theta_\gamma} I_\gamma(\frac{7}{2} \to \frac{3}{2})$	$I_\gamma(J_i \to J_f)/I_\gamma(\frac{7}{2} \to \frac{3}{2})$
$\frac{3}{2}$	$\frac{3}{2}$	460	0.033±0.004	0.050±0.016
$\frac{3}{2}$	$\frac{1}{2}$	387	0.012±0.004	
$\frac{3}{2}$	$\frac{5}{2}$	321	0.011±0.002	0.016±0.005
$\frac{3}{2}$	$\frac{3}{2}$	280	0.013±0.004	
$\frac{5}{2}$	$\frac{3}{2}$	559	0.044±0.006	0.167±0.023
$\frac{5}{2}$	$\frac{5}{2}$	420	0.021±0.004	0.070±0.018
$\frac{5}{2}$	$\frac{3}{2}$	234	0.012±0.004	0.067±0.013
$(\frac{7}{2})$	$\frac{5}{2}$	668	0.020±0.006	0.157±0.024
$(\frac{7}{2})$	$\frac{7}{2}$	449	0.010±0.003	0.124±0.020

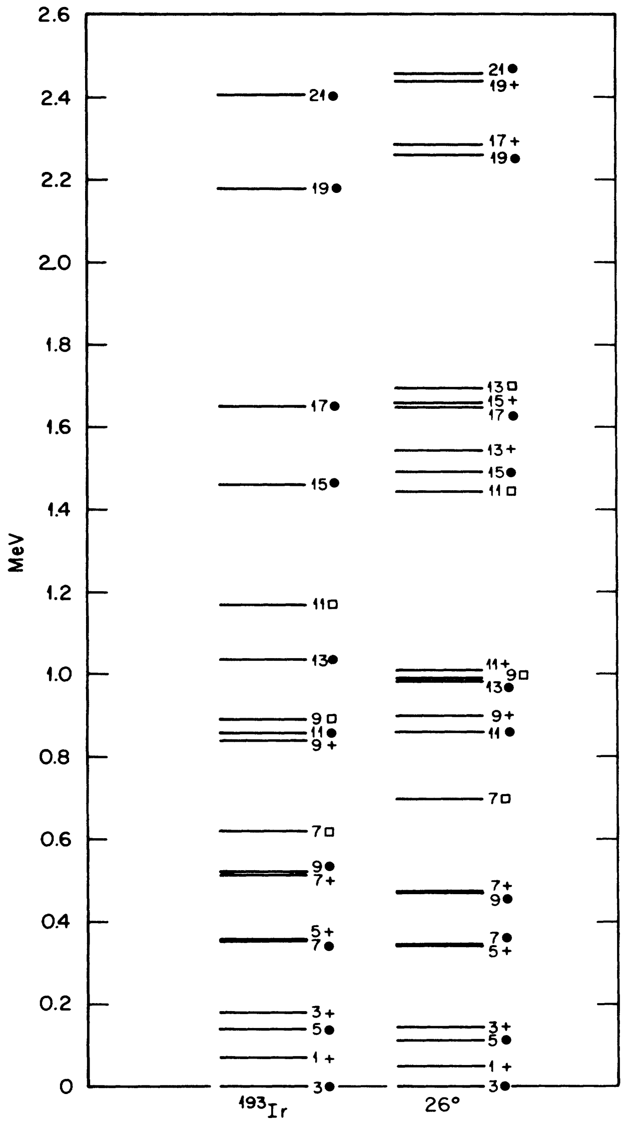

FIG. 2. Comparison of experimental levels in ^{193}Ir with those predicted from the particle-asymmetric-rigid-rotor model calculations for $\epsilon=0.15$, $\gamma=26°$, and $E(2^+)=210$ keV. Levels labeled with the symbols ●, +, and □ correspond to members of the $\frac{3}{2}^+$, $\frac{1}{2}^+$, and $\frac{7}{2}^+$ bands, respectively.

$$\mathrm{PAIR}=0.0900\ \mathrm{MeV}\ ,\quad PSD(1,1)=-0.1207\ \mathrm{MeV}\ ,$$

$$\mathrm{ELL}=0.0220\ \mathrm{MeV}\ ,\quad PDD(1,1)=-0.7043\ \mathrm{MeV}\ ,$$

$$\mathrm{QQ}=-0.0010\ \mathrm{MeV}\ ,\quad PDD(3,1)=-0.0396\ \mathrm{MeV}\ ,$$

$$\mathrm{OCT}=0.0050\ \mathrm{MeV}\ ,\quad EB=EF=0.1387\ e\,\mathrm{b}\ .$$

All of the other parameters were set to zero. The parameter χ, the coefficient of the $(d^\dagger\times\tilde{d})$ term in the $T^{(E2)}$ operator, was set equal to -1.0 in the numerical calculations. Figure 3 shows a comparison between the experimental energy levels of ^{193}Ir and the theoretical levels from the IBFA model. The lowest representation of the Spin(6) symmetry for ^{193}Ir with $N=7$ bosons and $M=1$ fermions is $\sigma_1=N+\frac{1}{2}=\frac{15}{2}$. The numbers in parentheses denote the Spin(5) labels (τ_1,τ_2). All of the states of the lowest Spin(5) representations $(\frac{1}{2},\frac{1}{2})$, $(\frac{3}{2},\frac{1}{2})$, and $(\frac{5}{2},\frac{1}{2})$ are observed in ^{193}Ir by Coulomb excitation. Seven of the eight states in the representation $(\frac{7}{2},\frac{1}{2})$ and two of the eleven states in the representation $(\frac{9}{2},\frac{1}{2})$ are also observed. The inset in Fig. 3 shows a few states in the next higher representation $\sigma_1=\frac{13}{2}$. The third $\frac{3}{2}$ state at 460 keV is associated with the representation $(\frac{1}{2},\frac{1}{2})$. The basis for this assignmentt comes from the ^{194}Pt(t,α)^{193}Ir reaction.[11] The average absolute deviation between experimental and theoretical energies from the IBFA model calculations is 66 keV for 16 states with $J\le\frac{11}{2}$. Only states with $J\le\frac{11}{2}$ were included in the numerical calculations for ^{193}Ir. In Fig. 3 the positions of the states with $J>\frac{11}{2}$ are from the calculations for ^{191}Ir.

Because of the strong correlation of the transition energies and the γ-ray yields for corresponding transitions in ^{191}Ir and ^{193}Ir in Table I, we do not present a detailed comparison of the yields for ^{193}Ir with model predictions via four figures as was done in Ref. 1. In any case, for five interband transitions originating in the $K=\frac{1}{2}^+$ and $\frac{7}{2}^+$ bands, the IBFA model would underestimate the γ-ray yields by one to two orders of magnitude. These interband transitions are $\frac{3}{2}'\to\frac{3}{2}$, $\frac{5}{2}'\to\frac{3}{2}$, $\frac{7}{2}'\to\frac{5}{2}$, $\frac{7}{2}''\to\frac{3}{2}$, and $\frac{9}{2}''\to\frac{7}{2}$ in Table I. Neither model offers a satisfactory description of the γ-ray yields from decay of the states in the $\frac{7}{2}^+$ rotational-like band. For example, the γ-ray yields for the transitions $\frac{7}{2}''\to\frac{3}{2}$ and $\frac{9}{2}''\to\frac{7}{2}$ are underestimated by both models.

A comparison of the experimental[6,12] and model-predicted $B(E2)$ values for ^{193}Ir is presented in Table III. The $B(E2)$'s for the decay modes of the Coulomb excited states are based on nuclear spectroscopic information.[6,7,13,14] Both models reproduce the $B(E2)$ values for the collective transitions with reasonable success. However, the IBFA model tends to underestimate the $B(E2)$ values of two moderately collective transitions by an order of magnitude, viz., the 180- and 621-keV transitions. These transitions are forbidden in the Spin(6) symmetry as they have $\Delta\tau_1=2$. The particle-asymmetric-rigid-rotor model prediction of the $E2/M1$ mixing ratio $\delta=-0.97$ for the $\frac{7}{2}''\to\frac{5}{2}$ transition of 482 keV gives an excellent account of the observed angular distribution for this transition. The lifetimes of the 460- and 559-keV states are known from ^{193}Ir(γ,γ) resonance fluorescence measurements by Metzger.[15] The $B(E2)$'s deduced from these data are included in Table III. There is excellent agreement between Coulomb excitation results and resonance fluorescence results.

Finally, Table IV presents a comparison of experimental and model-predicted $B(E2)$ values by U(6/20) and U(6/4) supersymmetry schemes for ^{193}Ir. For completeness, the results from the IBFA model [broken Spin(6)] and the particle-asymmetric-rigid rotor model calculations are included in Table IV. The selection rule $\Delta\tau_1$ for the $E2$ operator is the same in the U(6/20) and U(6/4) supersymmetry models of the odd-A nucleus. It should be

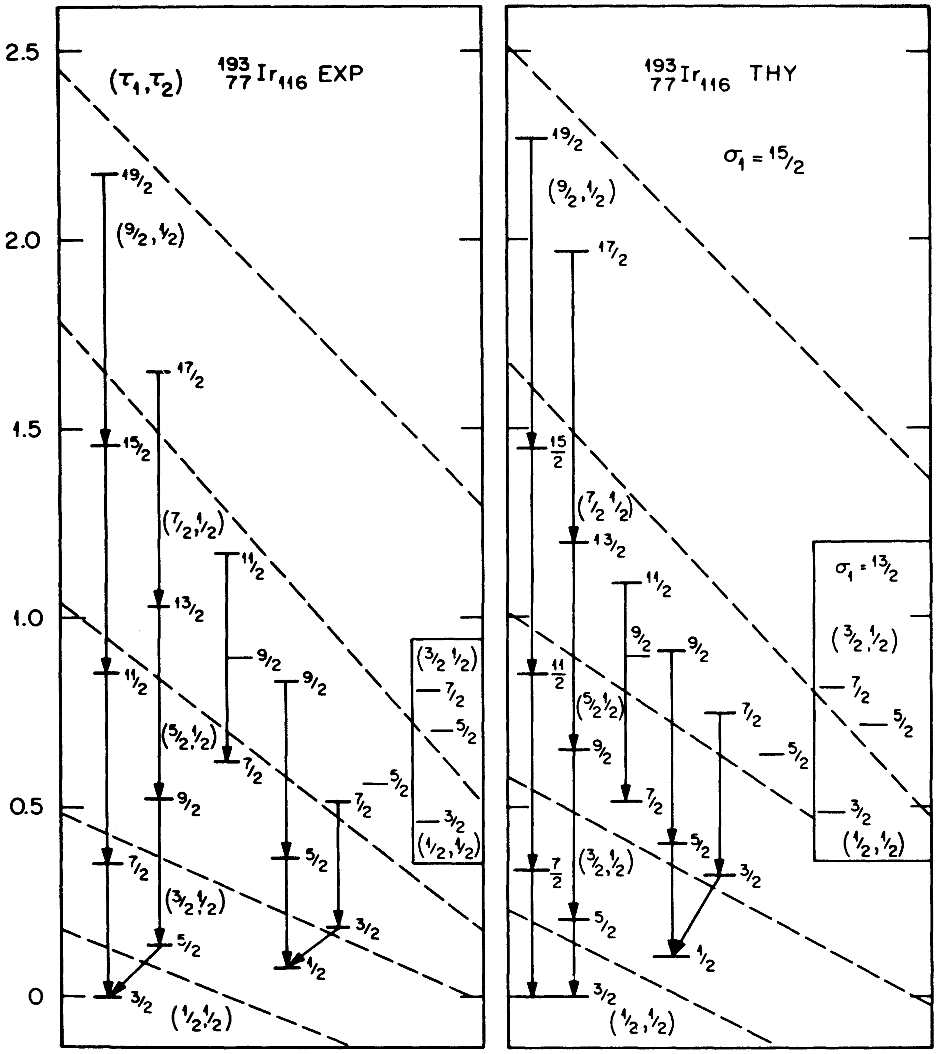

FIG. 3. Experimental level spectrum of ^{193}Ir and the theoretical levels from the IBFA model numerical calculations for the lowest representation of the Spin(6) symmetry. The numbers in parentheses denote the Spin(5) labels (τ_1,τ_2). The states of a given Spin(5) representation (τ_1,τ_2) are grouped between the dashed lines. The inset shows a few states in the next higher representation $\sigma_1=\frac{13}{2}$.

noted that a simplified form was chosen for the $T^{(E2)}$ operator,[4,5] namely $T^{(E2)}=\gamma G^{(2)}$, where γ is an adjustable constant and $G^{(2)}$ is a generator of the group Spin(6). The $B(E2)$ values predicted by U(6/20) and U(6/4) supersymmetry schemes differ by only about 25%. For both supersymmetry schemes there is a lack of detailed agreement with the $B(E2)$ values for the $\Delta\tau_1=1$ transitions from the decay of the $\tau_1=\frac{3}{2}$ states to the $\frac{3}{2}$ ground state. These features are, however, reproduced to a much better degree by the broken Spin(6) calculations. There is one transition $\frac{3}{2}'\rightarrow\frac{3}{2}$ of 180 keV in ^{193}Ir with a $B(E2,\frac{3}{2}'\rightarrow\frac{3}{2})=14B(E2)_{sp}$ which is a forbidden $\Delta\tau_1=2$ transition in both supersymmetry schemes. This moderately collective $E2$ transition is not a special situation in ^{193}Ir but a general feature in ^{191}Ir and ^{197}Au.[16] One would like to understand this in the context of supersymmetry and Spin(6) symmetry. In a weak-coupling scheme, the coupling of a $\frac{3}{2}^+$ ground state to the 2^+ state of the even-even core gives rise to a multiplet of states with $J=\frac{7}{2}^+$, $\frac{5}{2}^+$, $\frac{3}{2}^+$, and $\frac{1}{2}^+$. The observed $B(E2)$ values for deexcitation of these states in ^{197}Au is reproduced by the weak-coupling scheme.[16] On the other hand, Spin(6) symmetry corresponds to a strongly coupled scheme.[18] The "weak-coupling" $\frac{3}{2}^+$ state is missing in the $\tau_1=\frac{3}{2}$ multiplet. This state has been pushed up in energy by the boson-fermion interaction for Spin(6) by the quadrupole interaction term[11,18] to form the head of the next higher representation $\sigma_1=\frac{13}{2}$ and $\tau_1=\frac{1}{2}$. An appreciable reduction of the strength of the quadrapole interaction term in the case of ^{193}Ir would be in conflict with the $d_{3/2}$ spectroscopic strength observed from the ^{194}Pt(t,α)^{193}Ir reaction[11] and with the prediction of U(6/4) supersymmetry.

There are eight observed $\Delta\tau_1\geq 2$ transitions. Six of these are listed in Table IV and the other two interband transitions $\frac{7}{2}' \rightarrow \frac{5}{2}$ and $\frac{9}{2}'' \rightarrow \frac{7}{2}$ are listed in Table I. Aside from the 180- and 621-keV transitions, these $B(E2)_{\rm exp}$ range between 1.4 and 5.4 s.p.u., which are an order of magnitude smaller than the collective transitions. This means that the problems in the model calculations of noncollective $E2$ matrix elements are of the order of a few percent of the collective matrix elements. Besides

TABLE III. Experimental and model-predicted $B(E2)$ values for ^{193}Ir.

Initial state		Final state			$B(E2,J_i \rightarrow J_f)(e^2 b^2)$		
J_i	K_i	J_f	K_f	E_γ (keV)	Expt.[a]	Triaxial rotor	Broken Spin(6) IBFA
$\frac{11}{2}$	$\frac{3}{2}$	$\frac{7}{2}$	$\frac{3}{2}$	499	0.333±0.023[b]	0.450	0.421
$\frac{9}{2}$	$\frac{3}{2}$	$\frac{5}{2}$	$\frac{3}{2}$	382.9	0.496±0.018[b]	0.452	0.355
$\frac{7}{2}$	$\frac{3}{2}$	$\frac{3}{2}$	$\frac{3}{2}$	357.7	0.255±0.005	0.253	0.299
$\frac{7}{2}$	$\frac{3}{2}$	$\frac{5}{2}$	$\frac{3}{2}$	218.8	0.150±0.036	0.119	0.158
$\frac{5}{2}$	$\frac{3}{2}$	$\frac{3}{2}$	$\frac{3}{2}$	138.9	0.510±0.010	0.491	0.417
$\frac{3}{2}$	$\frac{3}{2}$	$\frac{3}{2}$	$\frac{3}{2}$	0.0	0.281±0.007[c]	0.209	0.355
$\frac{5}{2}$	$\frac{1}{2}$	$\frac{3}{2}$	$\frac{3}{2}$	361.8	0.0093±0.004	0.038	0.0003
$\frac{5}{2}$	$\frac{1}{2}$	$\frac{1}{2}$	$\frac{1}{2}$	289	0.47±0.08	0.228	0.258
$\frac{5}{2}$	$\frac{1}{2}$	$\frac{3}{2}$	$\frac{1}{2}$	182	0.19±0.04	0.021	0.0001
$\frac{3}{2}$	$\frac{1}{2}$	$\frac{3}{2}$	$\frac{3}{2}$	180	0.092±0.007	0.110	0.0018
$\frac{3}{2}$	$\frac{1}{2}$	$\frac{1}{2}$	$\frac{1}{2}$	107	$0.27^{+0.11}_{-0.09}$	0.274	0.181
$\frac{1}{2}$	$\frac{1}{2}$	$\frac{3}{2}$	$\frac{3}{2}$	73	0.274±0.032	0.095	0.217
$\frac{7}{2}$	$\frac{7}{2}$	$\frac{3}{2}$	$\frac{3}{2}$	621	0.0575±0.0020	0.0238	0.0005
$\frac{7}{2}$	$\frac{7}{2}$	$\frac{5}{2}$	$\frac{3}{2}$	482	0.135±0.020	0.094	0.189
$\frac{3}{2}''$	$\frac{1}{2}$	$\frac{3}{2}$	$\frac{3}{2}$	460	0.023±0.002[a,d,e]	0.042	0.0001
$\frac{3}{2}''$	$\frac{1}{2}$	$\frac{1}{2}$	$\frac{1}{2}$	387	0.00328±0.0026	0.037	0.0036
$\frac{3}{2}''$	$\frac{1}{2}$	$\frac{5}{2}$	$\frac{3}{2}$	321	0.0049±0.0017	0.031	0.0006
$\frac{3}{2}''$	$\frac{1}{2}$	$\frac{3}{2}$	$\frac{1}{2}$	280	$0.0014^{+0.0019}_{-0.0011}$	0.0018	0.074
$\frac{5}{2}''$	$\frac{3}{2}$	$\frac{3}{2}$	$\frac{3}{2}$	559	0.0136±0.0031[d,e]	0.0023	0.0001
$\frac{5}{2}''$	$\frac{3}{2}$	$\frac{5}{2}$	$\frac{3}{2}$	420	0.036±0.008	0.0039	0.0010
$\frac{5}{2}''$	$\frac{3}{2}$	$\frac{1}{2}$	$\frac{1}{2}$	486	0.028±0.014	0.0081	0.0097
$\frac{5}{2}'''$	$\frac{5}{2}$	$\frac{3}{2}$	$\frac{3}{2}$	695	0.0044±0.0015[e]		0.0004
$\frac{7}{2}'''$	$\frac{5}{2}$	$\frac{3}{2}$	$\frac{3}{2}$	807	0.0063±0.0021[e]	0.0065	0.0

[a]From Refs. 6 and 12 except if noted otherwise. Reference 6 also includes earlier Coulomb excitation results. Except for the 218.8- and 482-keV transitions the $E2/M1$ ratios are taken from Ref. 13.
[b]From Ref. 12.
[c]From Ref 14.
[d]From Ref. 15.
[e]From the present experiment.

these forbidden transitions, there are six transitions in Table IV with $\Delta\sigma_1=1$ which are forbidden in the U(6/20) and U(6/4) supersymmetry schemes (the $T^{(E2)}$ operator satisfies the selection rule $\Delta\sigma_1=0$). For all but one of these, the experimental $B(E2)$ values are less than one s.p.u. or the noncollective $E2$ matrix elements are $\sim 1\%$ of the collective matrix elements. The triaxial rotor model overestimates two of these noncollective transitions by an order of magnitude, viz., the 387-and 321-keV transitions. There is one collective transition, viz., the 182-keV intraband transition in the triaxial rotor scheme or the $\Delta\tau_1=0$ transition in the supersymmetry scheme, for

TABLE IV. Comparison between experimental and model-predicted $B(E2)$ values for ^{193}Ir. The $B(E2)$ values are given in units of $B(E2)_{sp}=0.00662$ e^2b^2 for $A=193$. The adjustable constant in the $E2$ operator deduced from $B(E2)_{exp}$ for ^{192}Os is $\gamma^2=3.32B(E2)_{sp}$. In U(6/20) $\sigma_1=\frac{17}{2}$ and in U(6/4) $\sigma_1=\frac{15}{2}$.

							$B(E2)$ calculated			
Nucleus	τ_{1i}	J_i	τ_{1f}	J_f	E_γ (keV)	$B(E2)_{exp}$	U(6/20)	U(6/4)	Broken Spin(6)	Triaxial rotor
^{193}Ir	$\frac{3}{2}$	$\frac{1}{2}$	$\frac{1}{2}$	$\frac{3}{2}$	73.0	41.4 ± 4.8	69	56	32.8	14.4
	$\frac{3}{2}$	$\frac{5}{2}$	$\frac{1}{2}$	$\frac{3}{2}$	138.9	77.0 ± 1.5	69	56	63.0	74.1
	$\frac{3}{2}$	$\frac{7}{2}$	$\frac{1}{2}$	$\frac{3}{2}$	357.7	38.5 ± 0.8	69	56	45.2	38.1
	$\frac{5}{2}$	$\frac{3}{2}$	$\frac{1}{2}$	$\frac{3}{2}$	180.0	13.9 ± 1.1	0.0	0.0	0.27	16.5
	$\frac{5}{2}$	$\frac{5}{2}$	$\frac{1}{2}$	$\frac{3}{2}$	361.8	1.40 ± 0.60	0.0	0.0	0.5	5.7
	$\frac{5}{2}$	$\frac{7}{2}$	$\frac{1}{2}$	$\frac{3}{2}$	621	8.7 ± 0.3	0.0	0.0	0.08	3.6
	$\frac{3}{2}$	$\frac{7}{2}$	$\frac{3}{2}$	$\frac{5}{2}$	218.8	22.7 ± 5.4	15.4	12.6	23.9	18.0
	$\frac{5}{2}$	$\frac{3}{2}$	$\frac{3}{2}$	$\frac{1}{2}$	107.0	$40.8^{+16.6}_{-13.6}$	32.5	25.9	27.3	41.3
	$\frac{5}{2}$	$\frac{5}{2}$	$\frac{3}{2}$	$\frac{1}{2}$	289	71.0 ± 12.1	55.8	44.4	39.0	34.5
	$\frac{5}{2}$	$\frac{7}{2}$	$\frac{3}{2}$	$\frac{5}{2}$	482	20.4 ± 3.0	47.4	37.7	28.5	14.1
	$\frac{5}{2}$	$\frac{9}{2}$	$\frac{3}{2}$	$\frac{5}{2}$	382.9	74.9 ± 2.7	73.0	58.1	53.6	68.3
	$\frac{5}{2}$	$\frac{11}{2}$	$\frac{3}{2}$	$\frac{7}{2}$	499	50.3 ± 3.5	93.0	74.0	78.7	68.0
$\sigma_{1i=13/2}$	$\frac{1}{2}$	$\frac{3}{2}$	$\frac{1}{2}$	$\frac{3}{2}$	460	3.5 ± 0.3	0.0	0.0	0.02	6.3
$\sigma_{1i=13/2}$	$\frac{1}{2}$	$\frac{3}{2}$	$\frac{3}{2}$	$\frac{1}{2}$	387	0.62 ± 0.41	0.0	0.0	0.54	5.6
$\sigma_{1i=13/2}$	$\frac{1}{2}$	$\frac{3}{2}$	$\frac{3}{2}$	$\frac{5}{2}$	321	0.74 ± 0.26	0.0	0.0	0.09	4.7
$\sigma_{1i=13/2}$	$\frac{1}{2}$	$\frac{3}{2}$	$\frac{5}{2}$	$\frac{3}{2}$	280	$0.21^{+0.29}_{-0.17}$	0.0	0.0	11.1	0.27
$\sigma_{1i=13/2}$	$\frac{3}{2}$	$\frac{5}{2}$	$\frac{3}{2}$	$\frac{1}{2}$	695	0.66 ± 0.23	0.0	0.0	0.060	
$\sigma_{1i=13/2}$	$\frac{3}{2}$	$\frac{7}{2}$	$\frac{1}{2}$	$\frac{3}{2}$	807	0.95 ± 0.23	0.0	0.0	0.0	1.0
	$\frac{5}{2}$	$\frac{5}{2}$	$\frac{5}{2}$	$\frac{3}{2}$	182	28.7 ± 6.0	1.8	1.4	0.02	3.2
	$\frac{7}{2}$	$\frac{5}{2}$	$\frac{1}{2}$	$\frac{3}{2}$	559	2.1 ± 0.5	0.0	0.0	0.015	0.35
	$\frac{7}{2}$	$\frac{5}{2}$	$\frac{3}{2}$	$\frac{5}{2}$	420	5.4 ± 1.2	0.0	0.0	0.15	0.59
	$\frac{7}{2}$	$\frac{5}{2}$	$\frac{3}{2}$	$\frac{1}{2}$	486	4.2 ± 2.1	0.0	0.0	1.5	1.2
	$\frac{1}{2}$	$\frac{3}{2}$	$\frac{1}{2}$	$\frac{3}{2}$	0.0	(42.4 ± 1.1)[a]	73	60	53.6	31.7
^{192}Os	1	2	0	0	205.8	(63.8 ± 0.6)[b]				

[a]Reference 14.
[b]Reference 17.

which the model predictions underestimate the $B(E2)$ value by at least one order of magnitude.

The $B(E3)$ for excitation of the negative-parity states extracted from the data is $(3.3\pm2.0)B(E3)_{sp}$. The $B(E3)$ for excitation of the 3^- state at 1341 keV in ^{192}Os is $(11.3\pm2.8)B(E3)_{sp}$, where $B(E3)_{sp}=1.53\times10^{-74}\ e^2\text{cm}^6$. This result was obtained from Coulomb excitation of ^{192}Os with 15-MeV ^{4}He ions.

IV. CONCLUSION

Prior to the present study, the experimental evidence present in support of supersymmetry in the Os—Ir nuclei has been limited. For example, only seven $B(E2)$ values were known for ^{193}Ir. From this study, it can be concluded that the more collective transitions, viz., $\Delta\tau_1=1$ transitions of the Spin(6) symmetry, are described reasonably well by the IBFA model calculations with broken Spin(6) symmetry and also by the supersymmetry schemes U(6/20) and U(6/4). A serious problem is the $\Delta\tau_1=2$ transition $\frac{3}{2}'\rightarrow\frac{3}{2}$ of 180 keV in ^{193}Ir with moderate collectivity which is forbidden in both supersymmetry models. This is not a special situation in ^{193}Ir but a general feature in ^{191}Ir and ^{197}Au. Because of the simple form chosen for the $E2$ transition operator, only small differences in the $B(E2)$ values are predicted by the U(6/20) and U(6/4) supersymmetry models. It remains to be seen if a more general form[18] of the $E2$ transistion operator would improve the description of the $B(E2)$ values in ^{193}Ir, in particular, a relaxation of the forbidden $\Delta\tau_1=2$ and $\Delta\sigma_1=1$ transitions. In general, we must conclude that the most successful interpretation of the experimental energies of the states and the $B(E2)$ values in ^{193}Ir is the particle-asymmetric-rigid-rotor model.

ACKNOWLEDGMENTS

We are indebted to F. Iachello for numerous discussions concerning the IBFA model, spinor symmetries, and supersymmetries and to F. Iachello and S. Kuyucak for the broken Spin(6) calculations of energies, and $E2$ and $M1$ matrix elements. We are extremely grateful to G. Leander for discussions and for supplying the code for the particle-asymmetric-rigid-rotor model, to W. B. Ewbank for discussions on the use of this program, to J. Saladin for communicating the $B(E2)$ values from light-ion Coulomb excitation which were used in the calculation of Coulomb excitation yields, and to A. Balantekin for stimulating discussions. Finally, we wish to thank R. Sayer for expanding the Winther—de Boer code to handle 40 J states. Oak Ridge National Laboratory is operated by Martin Marietta Energy Systems, Inc. for the U.S. Department of Energy under Contract No. DE-AC05-840R21400. Research at the University of Tennessee is supported by the U.S. Department of Energy under Contract No. DE-AS05-76ER04936. Research at the Lawrence Berkeley Laboratory is supported by the U.S. Department of Energy under Contract No. DE-AC03-76SF00098.

*Present address: Etudes et Productions, Schlumberger, Clamar, France.

[1]F. K. McGowan, N. R. Johnson, I. Y. Lee, W. T. Milner, C. Roulet, Y. A. Ellis-Akovali, R. M. Diamond, F. S. Stephens, and M. W. Guidry, Phys. Rev. C **33**, 855 (1986).

[2]Ch. Vieu, S. E. Larsson, G. Leander, I. Ragnarsson, W. De Wieclawik, and J. S. Dionisio, Z. Phys. A **290**, 301 (1979).

[3]F. Iachello and O. Scholten, Phys. Rev. Lett. **43**, 679 (1979).

[4]A. B. Balantekin, I. Bars, and F. Iachello, Nucl. Phys. **A370**, 284 (1981).

[5]Yin-Sheng Ling, Mei Zhang, Jing-Ming Xu, Michel Vallieres, Robert Gilmore, Da Hsuan Feng, and Hong-Zhou Sun, Phys. Lett. **148B**, 13 (1984).

[6]V. S. Shirley, Nucl. Data Sheets **32**, 593 (1981).

[7]E. W. Kleppinger and S. W. Yates, Bull. Am. Phys. Soc. **29**, 1049 (1984); E. W. Kleppinger, Ph.D. thesis, University of Kentucky, 1984.

[8]A. Winther and J. de Boer, in *Coulomb Excitation,* edited by K. Alder and A. Winther (Academic, New York, 1966), p. 303.

[9]S. E. Larsson, G. Leander, and I. Ragnarsson, Nucl. Phys. **A307**, 189 (1978). Computer code supplied by G. Leander.

[10]The results from the IBFA model calculations were supplied by F. Iachello and S. Kuyucak.

[11]J. A. Cizewski, D. G. Burke, E. R. Flynn, R. E. Brown, and J. W. Sunier, Phys. Rev. C **27**, 1040 (1983).

[12]J. X. Saladin, A. A. E. Hussein, C. Y. Chen, S. Sergiwa, and C. Kuo, Bull. Am. Phys. Soc. **27**, 705 (1982); A. A. E. Hussein, Ph.D. thesis, University of Pittsburgh, 1981.

[13]K. S. Krane, At. Data Nucl. Data Tables **18**, 137 (1976).

[14]Y. Tunaka, R. M. Steffen, E. B. Shera, W. Reuter, M. V. Hoehn, and J. D. Zumbro, Phys. Rev. Lett. **51**, 1633 (1983).

[15]F. R. Metzger, Phys. Rev. C **2**, 2024 (1970).

[16]F. K. McGowan, W. T. Milner, R. L. Robinson, and P. H. Stelson, Ann. Phys. (N.Y.) **63**, 549 (1971).

[17]M. V. Hoehn, E. B. Shera, H. D. Wohlfahrt, Y. Y. Yamazaki, R. M. Steffen, and R. K. Sheline, Phys. Rev. C **24**, 1667 (1981).

[18]F. Iachello and S. Kuyucak, Ann. Phys. (N.Y.) **136**, 19 (1981).